Langmuir

Article

pubs.acs.org/Langmuir

Optimization of DNA Hybridization Efficiency by pH-Driven Nanomechanical Bending

Jiayun Zhang,* Hans Peter Lang, Genki Yoshikawa,† and Christoph Gerber

Swiss Nanoscience Institute, University of Basel, Klingelbergstrasse 82, CH-4056 Basel, Switzerland

Supporting Information

ABSTRACT: The accessibility and binding affinity of DNA are two key parameters affecting the hybridization efficiency in surface-based biosensor technologies. Better accessibility will result in a higher hybridization efficiency. Often, mixed ssDNA and mercaptohexanol monolayers are used to increase the hybridization efficiency and accessibility of surface-bound oligonucleotides to complementary target DNA. Here, no mercaptohexanol monolayer was used. We demonstrate by differential microcantilever deflection measurements at different pH that the hybridization efficiency peaks between pH 7.5 and 8.5. At low pH 4.5, hydration and electrostatic forces led to tensile surface stress, implying the reduced accessibility of the bound ssDNA probe for hybridization. In contrast, at high pH 8.5, the steric interaction between neighboring ssDNA strands was decreased by higher electrostatic repulsive forces, bending the microcantilever away from the gold surface to provide more space for the target DNA. Cantilever deflection scales with pH-dependent surface hybridization efficiency because of high target DNA accessibility. Hence, by changing the pH, the hybridization efficiency is adjusted.

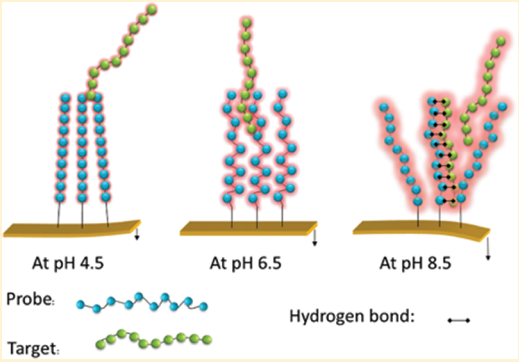

1. INTRODUCTION

DNA hybridization has been widely studied using current biosensing technologies such as DNA microarrays,[1] surface plasmon resonance (SPR),[2] quartz crystal microbalance (QCM),[3] X-ray photoelectron spectroscopy (XPS),[4] and microcantilever biosensors[5−10] for applied drug discovery, disease diagnosis, genome research, and gene expression. All of these techniques rely on a surface modified with single-strand DNA (ssDNA) monolayers to provide a compact platform for probing specific interactions with complementary target DNA in solution, resulting in a physical response due to the hybridization between target and surface-bound ssDNA. For surface-based hybridization, two key factors need to be addressed: (1) DNA target accessibility and (2) affinity to ssDNA probes tethered to the sensor surface. In general, greater accessibility should ultimately lead to higher hybridization efficiency and stronger signals. Accessibility mainly relies on the ssDNA coverage density[11] and conformation on the surface. In solution, the dependence of DNA melting points and renaturation melting points on pH was studied over the pH range of 5−9.85[12] Over the past few years, several investigations have been performed in order to identify major factors affecting hybridization on the surface using various techniques. Tarlov and co-workers[13−16] reported that the hybridization efficiency is decreased at high surface coverage. At lower coverage, probes absorb in different orientations on the surface, resulting in a lower hybridization efficiency. Similarly, at higher surface coverage, because of steric hindrance, the hybridization efficiency is also low. Therefore, the hybridization efficiency had to be improved by adding mixed monolayers of thiol ssDNA with mercaptohexanol, which can reduce steric crowding and electrostatic repulsion between neighboring ssDNA strands and increase the hybridization accessibility. Mercaptohexanol serves to prevent the nonspecific adsorption of ss-DNA, thus facilitating the hybridization of already-adsorbed ssDNA oligonucleotides with complementary DNA oligonucleotides.[17] However, when a cantilever sensing technique was used, the deflection signal magnitude decreased to 1 nm.[8] Shchepinov[18] and Peeters[19] use spacer molecules to reduce the steric hindrance at the support to improve the hybridization of immobilized ssDNA.

Microcantilever biosensors have rapidly attracted increasing amounts of attention[20−24] not only as a label-free detection method[8,25] but also because of their versatility and high sensitivity[9,21] by converting biochemical processes into nanomechanical bending.[26−28] Here, pH-dependent hybridization is optimized without the need to form mixed ssDNA assemblies involving mercaptohexanol monolayers or other modifications. By grafting ssDNA to the cantilever surface at high density ($\sim 10^{13}$ strands per cm^2), an initial bending profile is imposed on the cantilever by the formation of the ssDNA monolayer. The higher the surface density, the more likely it is that the molecules adapt a conformation with a higher degree of order, facilitating the measurement of conformational changes in ssDNA by nanomechanical bending.[24] Microcantilevers are a unique platform that provide direct information about

Received: December 22, 2011
Revised: March 21, 2012
Published: March 22, 2012

   dx.doi.org/10.1021/la205066h | *Langmuir* 2012, 28, 6494−6501

Table 1. ssDNA and dsDNA Sequences

name	type of DNA	sequence
ssBioB2plus	probe	5′-SH-$(CH_2)_6$-TGCTGTTTGAAGATGCTGGTAGAAGA-3′
ssBioB2plusC	complement	5′-TCTTCTACCAGCATCTTCAAACAGCA
ssUnsp	nonspecific reference	5′-SH-$(CH_2)_6$-ACACACACACACACACACACACACAC-3′
dsBioB2plus	probe	5′-SH-$(CH_2)_6$-TGCTGTTTGAAGATGCTGGTAGAAGA-3′
		3′-ACGACAAACTTCTACGACCATCTTCT-5′
dsUnsp	nonspecific reference	5′-SH-$(CH_2)_6$- ACACACACACACACACACACACAC -3′
		3′-TGTGTGTGTGTGTGTGTGTGTGTG-5′

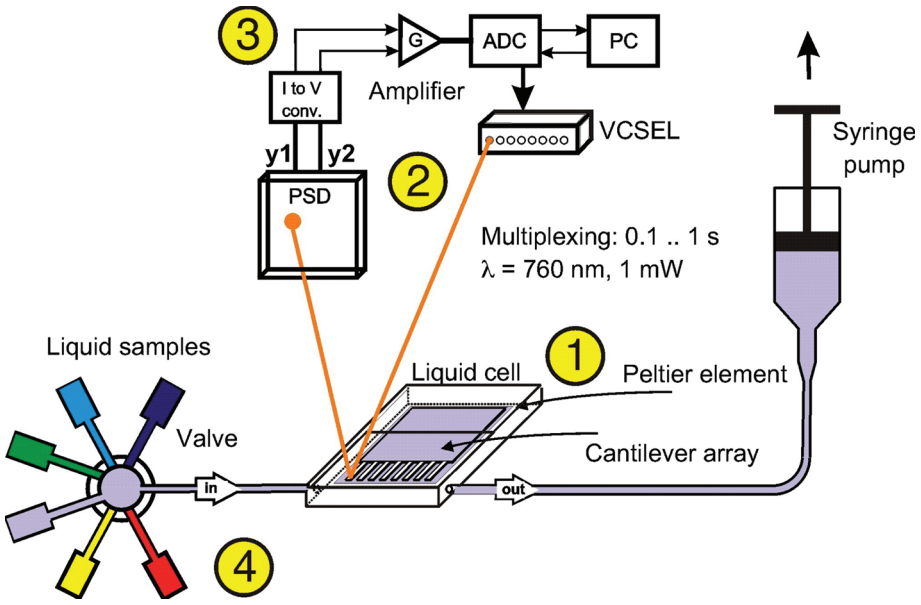

Figure 1. Schematic drawing of the measurement setup: (1) measurement chamber with a microcantilever array, (2) deflection readout system (optical beam deflection), (3) amplification electronics, (4) liquid-handling system,where the liquid is pulled out of individual reservoirs through the measurement chamber using a motorized syringe.

conformational changes in biomolecules (ssDNA, proteins, and polymers) whereas other methods provide only indirect evidence on conformational changes. Our results show fast and reversible mechanical bending responses due to conformational changes depending on the pH variation. Cantilever deflection scales with the pH-dependent surface hybridization efficiency due to high target DNA accessibility. The hybridization efficiency can be controlled by adjusting the pH.

2. EXPERIMENTAL SECTION

2.1.1. Materials. *ssDNA and dsDNA Sequences.* All thiol-modified (5′-SH-$(CH_2)_6$) single-stranded DNA (ssDNA) and double-stranded DNA (dsDNA) with 26 base pairs (Table 1) were obtained from Microsynth (Balgach, Switzerland). The nomenclature of the compounds refers to *Escherichia coli* biotin operon gene B, from which the sequences were taken. Prior to use, the thiol-modified ssDNA was extracted three times with the same volume of reagent-grade ethyl acetate, dried under vacuum at 40 °C for 4 to 5 h using a SpeedVac pump (TeleChem International, Inc., Sunnyvale, CA, USA). The concentrations of the purified thiol-modified ssDNA were determined by a biophotometer (Eppendorf AG, Germany) and calculated on the basis of the optical density (OD) of single-stranded DNA. (The ratio of the absorbance at 260 nm to that at 280 nm is ∼1.8 to 2.0.) The solution for functionalization consisted of purified thiol-modified ssDNA dissolved at a concentration of 40 μM in 50 mM triethyl ammonium acetate (TEAA) buffer.

2.1.2. Preparation of Buffers and Solutions. All buffers were prepared using HPLC-grade water from Fluka (Buchs, Switzerland). The buffer for functionalization was prepared at a concentration of 50 mM triethyl ammonium acetate (TEAA) buffer. Phosphate buffers (100 mM) were produced by mixing different ratios of 0.5 M monobasic and 0.5 M dibasic sodium phosphate stock solutions according to pH values of 4.5, 5.2, 6.5, 7.5, 8.5, and 9.5. The pH was confirmed with a pH meter (Inolab pH720, WTW GmbH, Germany) and adjusted with 0.1 M NaOH to pH 9.5. To ascertain that the pH-dependent DNA hybridization experiments do not exceed the buffering capacity of the sodium phosphate buffer, the pH was measured before and after the experiments, yielding the same pH value within 0.02 pH unit. The total ionic strength (300 mM) of each buffer was kept constant by adjusting the NaCl stock solution (1 M). The total ionic strength I is defined by

$$I = \frac{1}{2}\sum_{i=1}^{n} C_i Z_i^2 \qquad (1)$$

where C_i is the molar concentration of ion i and Z_i is the charge number of that ion. The sum is calculated over all ions in the solution. A 500 nM target complementary DNA solution was freshly prepared at each phosphate buffer pH. All solutions were filtered (0.2 μm filters, Sarsedt, Germany) and degassed prior to use. All chemicals were obtained from Fluka (Buchs, Switzerland).

2.2.1. Methods. *Cantilever Preparation.* Cantilever sensor arrays of eight identical silicon cantilevers with two solid bars[29] were fabricated at the IBM Zurich Research Laboratory. The size of the cantilever is 500 μm in length, 100 μm in width, and 0.9 μm in thickness. Prior to use, cantilever arrays are cleaned

dx.doi.org/10.1021/la205066h | Langmuir 2012, 28, 6494−6501

twice in freshly prepared piranha solution (H_2O_2/H_2SO_4 = 1:1) for 30 min, rinsed with Nanopure water and ethanol, and dried on a hot plate at 75 °C. A 2-nm-thick titanium layer and a 20-nm-thick gold layer were deposited onto one side of the cantilever array using an electron beam evaporator (EVA300, Alliance Concept, Cran Gevrier, France). Each of the freshly prepared gold-coated cantilever arrays was functionalized with five to six oligonucleotide probes and two to three reference oligonucleotides in a 40 μM solution of thiolated 26mer single-stranded oligodeoxyribonucleotide probe ssBioB2plus and nonspecific reference sequence ssUnsp in triethyl ammonium acetate buffer (TEAA, 50 mM), respectively. The density of tethered ssDNA probes for each individual cantilever array was observed to be 1.3 × 10^{13} probes/cm^2 by applying identical functionalization procedures and conditions as described previously.[8] The immobilized array was rinsed using 50 mM TEAA buffer and nanopure water and stored at 4 °C. We used various random arrangements of sensor and reference cantilevers to exclude possible artifacts from the location of sensor and reference cantilevers. However, the same results were obtained for different arrangements of sensor and reference cantilevers, proving that the location of the cantilevers does not affect the results.

2.2.2. Measurement Setup. Cantilever deflection measurements were carried out on a homemade microcantilever sensor array setup (SL NOSE) equipped with a 15 μL liquid cell (Figure 1). A functionalized ssDNA array was mounted at an angle of 11° toward the incoming laser beam in the liquid cell and monitored in situ using an optical beam deflection technique setup. We utilized time-multiplexed vertical cavity surface-emitting lasers (VCSEL, Avalon Photonics, Zurich, Switzerland) with a linear-position-sensitive detector (SiTek, Partille, Sweden). LabView software controls liquid handling via a syringe pump (GENIE, Kent Scientific Corp, Torrington, CT, USA), a six-way position valve selector (Rheodyne, Rohnert Park, CA, USA), temperature regulation at 22.00 ± 0.02 °C, and data acquisition and processing.

The bending signal was subsequently converted into a difference in surface stress between the upper and lower sides of the cantilever, $\Delta\sigma$, using the Stoney equation[30,31]

$$\Delta\sigma = \frac{1}{3}\left(\frac{t}{l}\right)^2\left(\frac{E}{1-\nu}\right)\Delta z \qquad (2)$$

where l is the effective length of the cantilever, t is the thickness (0.9 μm), and $E/(1-\nu)$ = 181 GPa is the ratio between the Young's modulus E and Poisson ratio ν of Si(100), which is invariant within the {100} planes. Δz is the absolute deflection at the free end of each cantilever. The direction of absolute deflection bending signals observed in the experiments implies compressive surface stress, determined by a heating test (Supporting Information) using a Peltier element located beneath the cantilever array. Because of the bimetallic effect on gold-coated microcantilevers, a negative deflection signal corresponds to the downward bending of the cantilever (compressive stress, bending away from the gold coating). A positive signal corresponds to the upward motion of the cantilever resulting from the development of tensile surface stress.

2.2.3. Sensor Chip Preparation and Surface Plasmon Resonance (SPR) Experiments. Surface plasmon resonance measurements were performed at 21C° on a Biacore X instrument (Biacore AB Uppsala, Sweden) equipped with two flow cells. A sensor chip (SIA Kit Au, GE Healthcare Biosciences AB, Sweden) was mounted in the instrument. One of the flow cells is used as a refererence (Fc1) for the subtraction of background signals of the bulk solutions or nonspecific binding; therefore, a 6-mercapto-1-hexanol solution with a concentration of 1 mM was first injected, forming a layer on the surface of the reference flow cell (Fc1). The surface of the other flow cell (Fc2) was then immobilized by injecting 30 μL of thiolated single-stranded DNA (ssBioB2plus) with a concentration of 40 μM in TEAA buffer (50 mM, pH 7.0) at a flow rate of 10 μL/min. Following immobilization, the system was thoroughly purged with degassed water in order to remove nonspecifically bound adsorbants from the sensor surface. A stable baseline was obtained, followed by injections of solutions with three different pH values (phosphate buffers at pH 4.5, 6.5, and 8.5, ionic strength 300 mM) into both flow cells at a flow rate of 10 μL/min. Data from the reference cell were subtracted from data obtained from the sample measurement cell.

3. RESULTS AND DISCUSSION

3.1. pH-Dependent Surface Hybridization. For a correct determination of surface stresses, it is of upmost importance to use the difference in the bending responses of specific sensor and nonspecific reference cantilevers. Hence, unwanted side effects such as temperature drift, nonspecific binding, and refractive index effects are canceled. Hybridization occurring on the cantilever surface gives rise to a compressive surface stress[5,8−10] that causes the cantilever to bend downward. For comparison at different pH values, it is essential that reference and sensor sequences are of the same length and have the experimental conditions, such as the surface density, buffer composition, and ionic strength are identical. The differential deflections extracted from the deflection difference of the ssDNA-probe-functionalized cantilever minus that of a non-complementary reference sequence yields the net stress change of the specific binding reaction (Figure 2). pH-dependent hybridization experiments were performed on 10 different nanomechanical cantilever arrays at pH 4.5, 5.2, 6.5, 7.5, 8.5, and 9.5, respectively. A constant flow (30 μL/min) of phosphate buffer with a total ionic strength of 0.3 M was established until equilibrium at 22 °C and a stable baseline was reached. A pH solution containing target DNA at a concentration of 500 nM was injected at the same flow rate for hybridization.

Figure 3 shows the differential deflection signals for hybridization as a function of pH. The buffer solution was adjusted with 0.5 M dibasic sodium phosphate and 0.5 M monobasic sodium phosphate, whereby only a small amount of 0.1 M NaOH was used for pH 9.5. According to Castelino et.al,[32] a total ionic strength of 0.3 M was selected and kept constant for all measurements. The data show clear evidence that the complementary target DNA hybridization depends critically on the pH of the solution. When the cantilever array was exposed to solutions of pH 4.5 or 5.2 (close to the isoelectric point), the phosphate backbone of ssDNA was partially protonated after equilibrium. Upon injecting target molecules at these pH values, the differential hybridization bending signals were observed to be around ∼2.4 ± 0.8 or 3.6 ± 1.1 nm (for pH 4.5 and 5.2, respectively), which corresponds to a compressive surface stress of ∼0.5 ± 0.2 or 0.7 ± 0.2 mN/m (relative to the response of the reference cantilever). This finding suggests that the hybridization affinity was very poor. The slightly increased hybridization bending signal of ∼5.4 ± 1.6 nm at pH 6.5 may be explained by a competition between the protonation/deprotonation of ssDNA phosphate groups. At pH 7.5, the hybridization affinity leads to a significant increase in cantilever bending, peaking at pH 8.5, resulting in a maximum bending deflection of ∼17.7 ± 2.1 nm (corresponding to a compressive surface stress of ∼3.5 ± 0.4 mN/m relative to the response of the reference cantilever). Indicated errors were determined from the standard deviation of the signal. The signal was increased by a factor of 5−8 compared to that at a low pH of 4.5−5.2. Above pH 8.5, at which the phosphate backbone is fully deprotonated, the bending signals were found to decrease again at pH 9.5. Furthermore, at very low and very

dx.doi.org/10.1021/la205066h | Langmuir 2012, 28, 6494−6501

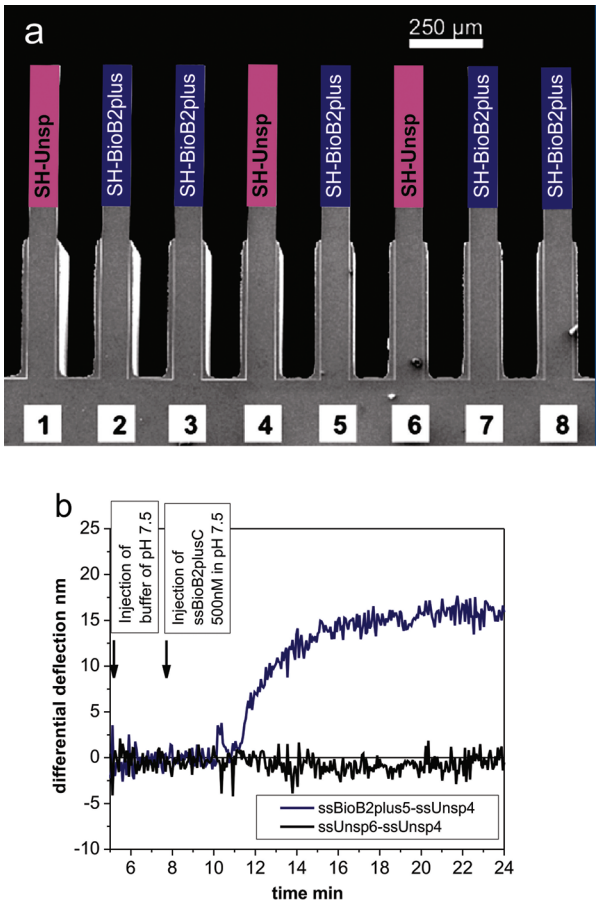

Figure 2. (a) Cantilever coatings in 1 out of 10 functionalized cantilever arrays (randomly selected). The cantilevers are individually functionalized with different sequences of thiol-functionalized ssDNA using microcapillaries as described in Table 1. The cantilevers measure 500 μm in length, 100 μm in width, and 0.9 μm in thickness. In the experiments, various random arrangements of sensor and reference cantilevers have been utilized to exclude possible artifacts from the locations of the sensor and reference cantilevers. (b) The difference in responses between a sensor and a reference cantilever (blue curve) shows the response represented by the bar displayed in dark blue at pH 7.5 in Figure.3. The black curve shows the difference in the responses of two reference cantilevers, yielding no signal.

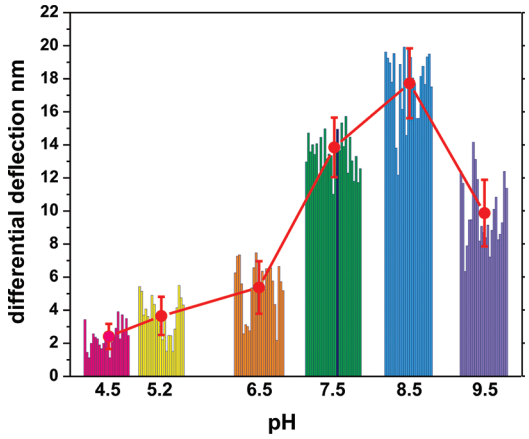

Figure 3. Each bar represents an independent measurement of the difference in responses of a sensor and a reference cantilever. Measurements were performed on 10 different arrays. The average of responses at a particular pH value is marked by a red dot and a standard deviation error bar. Because the differential nanomechanical response is a measure of the hybridization efficiency, we identify an optimized range for the hybridization efficiency of between 7.5 and 8.5, corresponding to physiological conditions.

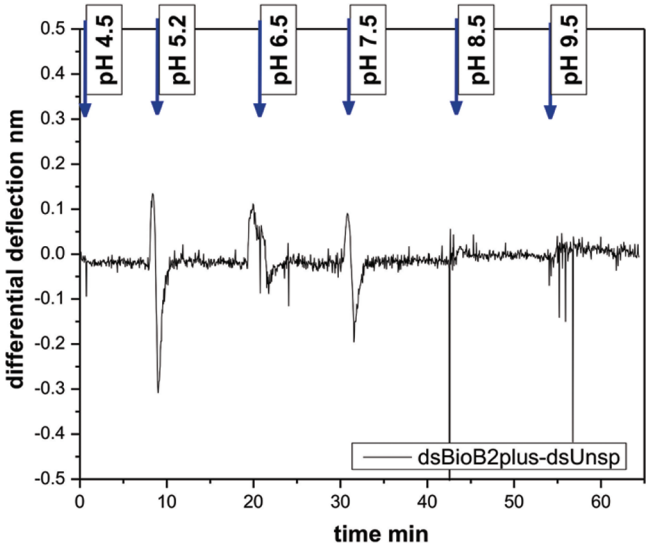

Figure 4. Control experiment with double-stranded DNA clearly showing that cantilever deflection does not depend on pH, validating the results displayed in Figure 3.

high pH, dsDNA denaturation occurs, being the main reason for the lower hybridization efficiency observed at very low and high pH.

We concluded from this experiment that the pH of a solution played a major role in the process of DNA hybridization on surfaces and that the hybridization efficiency was drastically lower at low pH.

The pH dependence of double-strand DNA micromechanical bending was investigated at pH 4.5, 5.2, 6.5, 7.5, 8.5, and 9.5 (0.3 M NaCl). Injection sequences of pH 4.5 buffer, followed by buffer injections with increasing pH, served as another important control experiment. Figure 4 shows differential measurements made on a cantilever array comprising four dsBioB2plus-functionalized and two dsUnsp-functionalized cantilevers. With increasing buffer pH, the differential deflection showed no dependence on pH. Injection spikes are due to the refractive index change during buffer injections.

3.2. Conformational Changes in ssDNA in Response to pH Variation. To shed light on the previous findings, we further investigated the effect of pH on the conformational changes in ssDNA. Three probe cantilevers were coated with a 26-mer sequence of ssDNA (ssBioB2plus), which was used as the probe in the previous hybridization measurements. Two cantilevers were functionalized with a thiolated 12-mer sequence of ssDNA (5′-SH-$(CH2)_6$-TGCTGTTTGAAG-3′, ssBioB2) that was selected for two reasons: (1) as a coating for the reference cantilevers in differential measurements and (2) as a sequence with a shorter chain length compared to the probe sequence in absolute deflection measurements. The structure of ssBioB2plus was designed by analogy to the sequence of ssBioB2. It consists of two parts, the first being identical to ssBioB2 with an alkanethiol linker at the 5′ end and the second being an extended "plus" part at the 3′ end. It is important to note that the surface density for both ssDNA's was

dx.doi.org/10.1021/la205066h | Langmuir 2012, 28, 6494–6501

obtained by using identical immobilization conditions for all cantilevers.

Three different sodium phosphate solutions (pH 6.5, 4.5, and 8.5) were reversibly cycled by sequential injections. Figure 5

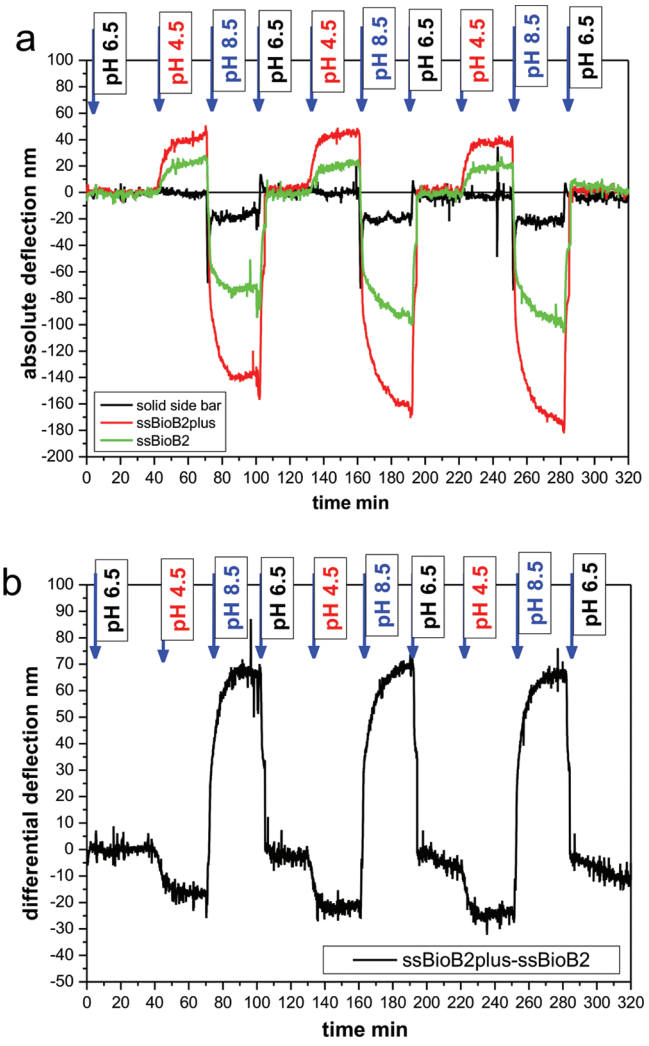

Figure 5. pH-induced surface bending measurements for cantilevers coated with 26-mer ssDNA (ssBioB2plus) and 12-mer ssDNA (ssBioB2) as well as a solid side bar. (a) Absolute deflection measurements obtained from three successive pH cycles. In each cycle, sodium phosphate buffer solutions with corresponding pH values (total ionic strength 0.3M) were injected (pH 6.5, 4.5, and 8.5 under a constant flow of 30 μL/min). Recurring injections of pH 6.5 phosphate solution served as an important control for the reversibility of the deprotonation/protonation reactions. A slight drift of the base lines of ssBioB2plus and ssBioB2 relative to the solid bar response baseline is observed. This effect is canceled in the differential deflection data. (b) Differential deflection measurements (ssBioB2-plus−ssBioB2).

shows the absolute and differential deflection measurements with three cycles of pH 6.5, 4.5, and 8.5, respectively, taken on a microcantilever array comprising three 26-mer ssDNA sequence coated cantilevers, two 12-mer ssDNA coated references, and one solid side bar used to monitor the change in refractive index during injections. The deflection at pH 6.5 (close to the pK_a of ssDNA on the surface)[7] was chosen as a baseline.

Figure 5a shows a direct observation of the conformational changes in ssDNA found in the absolute deflection signal (absolute motion of cantilevers). The titration measurements were started close to the pK_a of ssDNA on the surface at pH 6.5 in the sodium phosphate solution flow. It was found that upon decreasing the pH from 6.5 to 4.5 the absolute bending signals for both ssBioB2plus and ssBioB2 cantilevers were positive, which implies tensile surface stress. The average absolute response of ssBioB2plus (42.9 ± 3.1 nm) corresponds to a stronger upward bending than that of ssBioB2 (23.4 ± 2.3 nm). When solutions of increasingly higher pH values from 4.5 to 8.5 were injected, the absolute bending signals for both ssBioB2plus (−166.6 ± 13.4 nm) and ssBioB2 (−95.9 ± 6.5 nm) cantilevers show negative values corresponding to a compressive surface stress. The difference in absolute bending responses (averaged) between the ssBioB2plus cantilevers (red curve) and the ssBioB2 cantilevers (green curve) is evident. Longer ssDNA molecules produce larger absolute deflections than do shorter ones. When the pH was changed to 6.5, starting with the second and third cycles, the same bending profiles as in the first run were observed. We used a rigid bar located next to the flexible cantilevers to determine the amount of refractive index contribution to the cantilever bending signal. At pH 8.5, the influence of the refractive index due to the alkaline ions contained in the pH 8.5 solution is lower by a factor 4 to 7 than the cantilever deflection signals, thus the subtraction of the refractive index contribution ensures the validity of the cantilever deflection responses. The refractive index response (black line) represents only a virtual signal[20] measured on the solid bar during three pH cycles. Here, differential deflection data (ssBioB2plus−ssBioB2) were calculated by subtracting the response of the reference cantilever from the ssBioB2plus response (Figure 5b). This procedure allows us to eliminate bulk solution refractive index effects, nonspecific binding, and temperature drift. In the differential response signal, the extended "plus" part of ssBioB2plus conformational changes on the surface of the cantilever is observed directly.

The differential bending signal at pH 6.5 exhibits a stable baseline. Upon switching to a solution of pH 4.5, we found the corresponding differential deflection signals (−20.7 ± 2.9 nm) associated with ssBioB2plus protonation to reveal a net tensile surface stress. When a solution with a higher pH of 8.5 was injected, a differential bending signal (−67.8 ± 1.5 nm) was observed, corresponding to compressive surface stress. When the pH was changed back to a value of 6.5, the differential deflection was observed to return to the baseline. Three consecutive pH cycles reproducibly revealed surface conformational changes associated with changes in the pH environment. Protonation from pH 6.5 to 4.5 generated an average bending of 20.7 ± 2.9 nm. This bending signal corresponds to a tensile surface stress change of 4.0 ± 0.6 mN/m relative to the response of the reference cantilever. Changing the pH from 4.5 to 8.5 generated an average bending of 67.8 ± 1.5 nm, which corresponds to a compressive surface stress of 13.2 ± 0.3 mN/m relative to the response of the reference cantilever.

The parallel SPR measurement of pH-dependent conformational changes on ssDNA is shown in Figure 6, displaying SPR sensorgrams (RU) of ssDNA when varying the buffer pH from 6.5 to 4.5 to 8.5. When a pH 6.5 buffer was injected, the differential response was 48.8 ± 0.5RU. Upon changing the pH to 4.5, the signal decreased to 37.5 ± 0.2 RU, resulting in a change in 11.3 ± 0.7 RU. Changing the pH from 4.5 to 8.5 generated a shift of 19.57 ± 1.0 RU. Such successive cycles of

dx.doi.org/10.1021/la205066h | *Langmuir* 2012, 28, 6494−6501

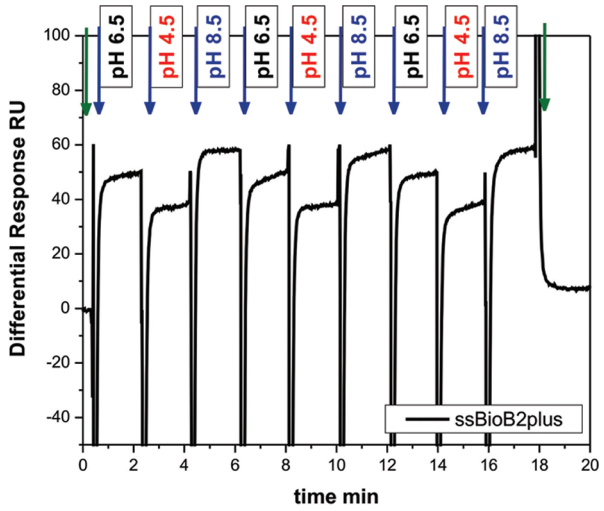

Figure 6. pH-induced SPR measurements using sensor chip coated with 26-mer ssDNA (ssBioB2plus). Sensorgrams were obtained from three successive pH cycles. In each cycle, sodium phosphate buffer solutions with corresponding pH values (total ionic strength 0.3 M) were injected (pH 6.5, 4.5, and 8.5) under a constant flow (flow rate 10 μL/min). The pH-dependent response of ssDNA confirmed the findings obtained with cantilevers in Figure 5. Injection spikes are due to the differing refractive index of water that was used instead of running buffer (green arrow).

pH indirectly revealed surface conformational changes that are consistent with the experimental results obtained directly via surface stress measurements with the cantilever method.

DNA surface hybridization is different from hybridization in solution where DNA probes are free to encounter their targets. The ssDNA probes are fixed at one end using a thiol anchor. The target complement molecules bind to them and become part of the DNA monolayer. Surface hybridization is governed by the 2D nature of the immobilized layer, involving effects of molecular charge and conformation, which impact the hybridization behavior in various ways. At constant surface density, the binding of probe ssDNA is dominated by two key factors: the first is the accessibility of target molecules in the probe monolayer, and the second is the binding affinity between probe and target molecules. pH-induced conformational changes on an ssDNA-functionalized surface result in changes in the nanomechanical bending signal of microfabricated cantilevers. The results of pH-dependent surface hybridization obtained using reference cantilevers (immobilized with non-complementary sequence ssUnsp, which did not hybridize with the probe tethered to the cantilever) were found to depend critically on the pH. Our findings show that the DNA surface hybridization affinity is associated to a large extent with conformational changes in ssDNA at the surface, depending on pH variations.

Figure 7 illustrates the conformational changes in ssDNA as a function of the increasing pH of sodium phosphate solution and the effect of the pH change on the surface hybridization affinity and depicts the surface response of ssDNA to three different pH environments before and after hybridization. Figure 7a shows that at low pH 4.5 protonation is driven by H^+ penetrating the monolayer of ssDNA, whereby the replacement of Na^+ is favored.[33] Hence, the repulsive hydration force between phosphate groups on neighboring probe molecules is reduced. An attractive force corresponding to a tensile stress resulted from steric crowding and dipole−dipole interactions. This suggests that at this pH the ssDNA chains are stretched by protonation. Therefore, the accessibility of the target molecules to the ssDNA monolayer is decreased and the hybridization affinity is poor. A similar effect was observed in synthetic polyelectrolyte brushes.[34]

To reduce steric effects on hybridization on planar surfaces, the pH can be increased to separate the probes physically through the bending of the cantilever surface. At high pH 8.5, a strong binding affinity between targets and probes was observed (large differential deflection signals, Figure 3). The proposed mechanism explains the high affinity due to the fact that the charged phosphate backbones of ssDNA strands being are fully deprotonated. The electrostatic repulsive force between strands could bend the cantilever downward and therewith generate a compressive surface stress that will diminish the steric effect and allow the target molecules to access the surface of ssDNA more easily. Close to the pK_a of ssDNA on the surface at pH 6.5, the charged phosphate backbone of ssDNA is partially protonated, having an isoelectric point of about 5.0.[35] DNA molecules are negatively charged because of phosphate groups if the pH is higher than the isoelectric point. Therefore, the electrostatic repulsive forces are still dominant between ssDNA strands, leading to compressive stress in comparison to the situation at pH 4.5. Above pH 8.5, the phosphate backbone of ssDNA is deprotonated and the bases of ssDNA are partially deprotonated. Although the accessibility of target molecules to the probe layer is high, the binding affinity is low, resulting in observed small (tensile) stress values relative to the response of the reference cantilever.

4. CONCLUSIONS

We have demonstrated rapid, reversible nanomechanical responses driven by pH-induced conformational changes in ssDNA on the surfaces of microcantilevers. Experiments on cantilevers differ from traditional assays in a distinct way: because cantilevers are flexible beams, mechanical issues during hybridization can be studied, including the development of and change in surface stress. The main advantages to using the cantilever technique comprise the following aspects: (1) new parameters such as the surface stress evolvement can be studied and (2) no mixed monolayer of molecules is required, leading to simpler and more reliable sample preparation.

We found that the nanomechanical bending motion and direction can be adjusted by changing the pH. In addition, the observation of pH-dependent surface hybridization on microcantilevers has proven that the accessibility and affinity of target molecules are governed by the interaction force and steric hindrance between the neighboring ssDNA strands on the microcantilever surface. Our findings reveal that pH plays a major role in the generation of the nanomechanical surface stress of hybridization. An optimized pH range for hybridization can be used to improve the sensitivity of DNA-based microcantilever array sensors and increase the accessibility to and affinity for ssDNA with respect to their complements during hybridization and to provide detailed information on the fundamental understanding of the role of surface stress. Selecting the pH value during surface hybridization allows us to maximize the hybridization efficiency.

dx.doi.org/10.1021/la205066h | *Langmuir* 2012, 28, 6494−6501

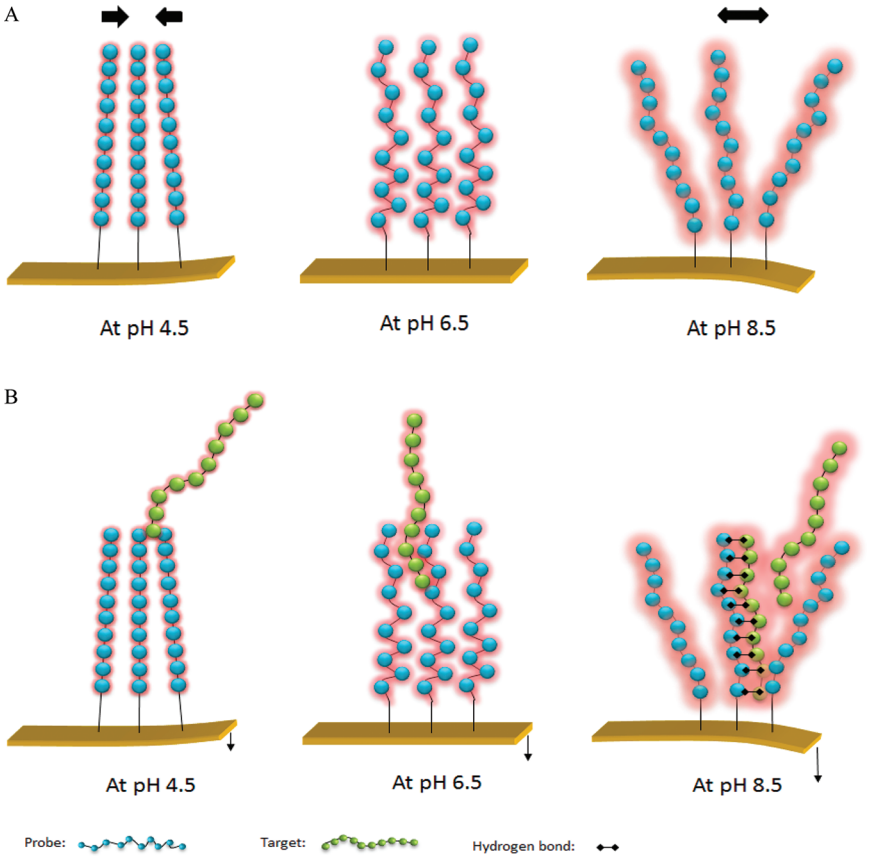

Figure 7. Schematic drawing illustrating (A) conformational changes in ssDNA immobilized on the surface of a cantilever in various pH environments (low, neutral, and high). Black double arrows indicate the interaction forces. At low pH 4.5, an attractive electrostatic force due to partial protonation acts on the ssDNA strands. The beginning of deprotonation sets in close to the pK_a of ssDNA on the surface at pH 6.5, which is beyond the isoelectric point. At high pH 8.5 ,ssDNA strands are fully deprotonated and the separation between strands increases because of electrostatic repulsion forces. (B) The pH-induced surface hybridization affinity depends on conformational changes in the ssDNA chains. ssDNA molecules are shown in blue, and the target complementary strands are shown in green. At low pH 4.5, the accessibility of ssDNA chains is low, resulting in a low hybridization efficiency. Close to the pK_a of ssDNA on the surface at pH 6.5, the ssDNA strands are more accessible to their complements, yielding a higher hybridization efficiency. At high pH 8.5, the steric hindrance is low and the hybridization efficiency is high. Clouds of negative charge are depicted as a red "glow" around the molecules.

■ ASSOCIATED CONTENT

Ⓢ Supporting Information

Peltier test. This material is available free of charge via the Internet at http://pubs.acs.org.

■ AUTHOR INFORMATION

Corresponding Author

*E-mail: jiayun.zhang@unibas.ch.

Present Address

[†]International Center for Materials Nanoarchitectonics (MANA), National Institute for Materials Science (NIMS), 1-1 Namiki, Tsukuba, Ibaraki 305-0044, Japan.

Notes

The authors declare no competing financial interest.

■ ACKNOWLEDGMENTS

We thank Dr. Rachel A. McKendry (UCL) and Dr. Joseph W. Ndieyira (Jomo Kenyatta University of Science and Agriculture) for valuable discussions. We also thank Dr. Larisa Kapinos (Biocenter, University of Basel) for assistance with the SPR measurements. The National Center of Competence for Nanoscale Science (NCCR Nano), the Swiss Nano Institute (SNI), and the Swiss National Science Foundation are acknowledged for financial support.

■ REFERENCES

(1) Woody, O. Z.; Doxey, A. C.; McConkey, B. J. Assessing the Evolution of Gene Expression Using Microarray Data. *Evol. Bioinf.* **2008**, *4*, 139.

(2) Su, X.; Wu, Y.; Knoll, W. Comparison of Surface Plasmon Resonance Spectroscopy and Quartz Crystal Microbalance Techniques for Studying DNA Assembly and Hybridization. *Biosens. Bioelectron.* **2005**, *21*, 719.

(3) Wong, E. L. S.; Chow, E.; Gooding, J. J. DNA Recognition Interfaces: The Influence of Interfacial Design on the Efficiency and Kinetics of Hybridization. *Langmuir* **2005**, *21*, 6957.

(4) Dekeyser, C. M.; Buron, C. C.; Mc Evoya, K.; Dupont-Gillain, C. C.; Marchand-Brynaert, J.; Jonasc, A. M.; Rouxhet, P. G. Oligo-(ethylene glycol) Monolayers by Silanization of Silicon Wafers: Real Nature and Stability. *J. Colloid Interface Sci.* **2008**, *324*, 118.

(5) Fritz, J.; Baller, M. K.; Lang, H. P.; Rothuizen, H.; Vettiger, P.; Meyer, E.; Guntherodt, H.-J.; Gerber, C.; Gimzewski, J. K. Translating Biomolecular Recognition into Nanomechanics. *Science* **2000**, *288*, 316.

(6) Mertens, J.; Rogero, C.; Calleja, M.; Ramos, D.; Martin-Gago, J. A.; Briones, C.; Tamayo, J. Label-Free Detection of DNA Hybridization Based on Hydrationinduced Tension in Nucleic Acid Films. *Nat. Nanotechnol.* **2008**, *3*, 301.

(7) Shu, W.; Liu, D.; Watari, M.; Riener, C. K.; Strunz, T.; Welland, M. E.; Balasubramanian, S.; McKendry, R. A. DNA Molecular Motor Driven Micromechanical Cantilever Arrays. *J. Am. Chem. Soc.* **2005**, *127*, 17054.
(8) McKendry, R. A.; Zhang, J.; Arntz, Y.; Strunz, T.; Hegner, M.; Lang, H.-P.; Baller, M. K.; Certa, U.; Meyer, E.; Guntherodt, H.-J.; Gerber, C. Multiple Label-Free Biodetection and Quantitative DNA-Binding Assays on a Nanomechanical Cantilever Array. *Proc. Natl. Acad. Sci. U.S.A.* **2002**, *99*, 9783.
(9) Zhang, J.; Lang, H.- P.; Huber, F.; Bietsch, A.; Grange, W.; Certa, U.; McKendry, R. A.; Guntherodt, H. J.; Hegner, M.; Gerber, C. Rapid and Label-Free Nanomechanical Detection of Biomarker Transcripts in Human RNA. *Nat. Nanotechnol.* **2006**, *1*, 214.
(10) Bietsch, A.; Zhang, J.; Hegner, M.; Lang, H.-P.; Gerber, C. Rapid Functionalization of Cantilever Array Sensors by Inkjet Printing. *Nanotechnology* **2004**, *15*, 873.
(11) Peterson, A. W.; Heation, R. J.; Giorgiadis, R. M. Rapid Functionalization of Cantilever Array Sensors by Inkjet Printing. *Nucleic Acids Res.* **2001**, *29*, 5163.
(12) Wetmur, J. G.; Davidson, N. Kinetics of Renaturation of DNA. *J. Mol. Biol.* **1968**, *31*, 349.
(13) Herne, T. M.; Tarlov, M. J. Article Characterization of DNA Probes Immobilized on Gold Surfaces. *J. Am. Chem. Soc.* **1997**, *119*, 8916.
(14) Steel, A. B.; Herne, T. M.; Tarlov, M. Electrochemical Quantitation of DNA Immobilized on Gold. *Anal. Chem.* **1998**, *70*, 4670.
(15) Steel, A. M.; Levicky, R.; Herne, T. M.; Tarlov, M. J. Immobilization of Nucleic Acids at Solid Surfaces: Effect of Oligonucleotide Length on Layer Assembly. *Biophys. J.* **2000**, *79*, 975.
(16) Opdahl, A.; Petrovykh, D. Y.; Kimura-Suda, H.; J. Tarlov, M. J.; Whitman, L. J. Independent Control of Grafting Density and Conformation of Single-Stranded DNA Brushes. *Proc. Natl. Acad. Sci. U.S.A.* **2007**, *104*, 9.
(17) Peterlinz, K. A.; Georgiadis, R. M.; Herne, T. M.; Tarlov, M. J. Observation of Hybridization and Dehybridization of Thiol-Tethered DNA Using Two-Color Surface Plasmon Resonance Spectroscopy. *J. Am. Chem. Soc.* **1997**, *119*, 3401.
(18) Shchepinov, M. S.; Case-Green, C.; Southern, E. M. Steric Factors Influencing Hybridisation of Nucleic Acids to Oligonucleotide Arrays. *Nucleic Acids Res.* **1997**, *25*, 1155.
(19) Peeters, S.; Stakenborg, T.; Reekmans, G.; Laureyn, W.; Lagae, L.; Van Aerschot, A.; Van Ranst, M. Impact of Spacers on the Hybridization Efficiency of Mixed Self-Assembled DNA/Alkanethiol Films. *Biosens. Bioelectron.* **2008**, *24*, 72.
(20) Koser, J.; Gaiser, S.; Muller, B. Contractile Cell Forces Exerted on Rigid Substrates. *Eur. Cell Mater.* **2011**, *21*, 479.
(21) Gruber, K; Horlacher, T.; Castelli, R.; Mader, A.; Seeberger, P. H.; Hermann, B. A. Cantilever Array Sensors Detect Specific Carbohydrate-Protein Interactions with Picomolar Sensitivity. *ACS Nano* **2011**, *5*, 3670.
(22) Zhang, N.-H.; Chen, J-Z; Li, J.-J.; Tan, Z.-Q. Mechanical Properties of DNA Biofilms Adsorbed on Microcantilevers in Label-Free Biodetections. *Biomaterials* **2010**, *31*, 6659.
(23) Zhang, N.-H.; Shan, J.-Y. An Energy Model for Nanomechanical Deflection of Cantilever-DNA Chip. *J. Mech. Phys. Solids* **2008**, *56*, 2328.
(24) Mertens, J.; Tamayo, J.; Kosaka, P.; Calleja, M. Observation of Spermidine-Induced Attractive Forces in Self-Assembled Monolayers of Single Stranded DNA Using a Microcantilever Sensor. *Appl. Phys. Lett.* **2011**, *98*, 153704.
(25) Yue, M.; Stachowiak, J. C.; Lin, H.; Datar, R.; Cote, R.; Majumdar, A. Label-Free Protein Recognition Two-Dimensional Array Using Nanomechanical Sensors. *Nano Lett.* **2008**, *8*, 520.
(26) Wu, G; Ji, H.; Hansen, K.; Thundat, T.; H.; Datar, R.; Cote, R.; Hagan, M. F.; Chakraborty, A. K.; Majumdar, A. Origin of Nanomechanical Cantilever Motion Generated from Biomolecular Interactions. *Proc. Natl. Acad. Sci. U.S.A.* **2001**, *98*, 1560.
(27) Stachowiak, J. C.; Yue, M.; Castelino, K.; Chakraborty, A.; Majumdar, A. Chemomechanics of Surface Stresses Induced by DNA Hybridization. *Langmuir* **2006**, *22*, 263.
(28) Watari, M.; Galbraith, J.; Lang, H.-P.; Sousa, M.; Hegner, M.; Gerber, C.; Horton, M. A.; McKendry, R. A. Investigating the Molecular Mechanisms of In-Plane Mechanochemistry on Cantilever Arrays. *J. Am. Chem. Soc.* **2007**, *129*, 601.
(29) Huber, F.; Lang, H.-P.; Hegner, M.; Despont, M.; Drechsler, U.; Gerber, C. Analyzing Refractive Index Changes and Differential Bending in Microcantilever Arrays. *Rev. Sci. Instrum.* **2008**, *79*, 086110.
(30) Stoney, G. G. The Tension of Metallic Films Deposited by Electrolysis. *Proc. R. Soc. London, Ser. A* **1909**, *82*, 172.
(31) Brantly, W. A. Calculated Elastic Constants for Stress Problems Associated with Semiconductor Devices. *J. Appl. Phys.* **1973**, *44*, 534.
(32) Castelino, K.; Kannan, B.; Majumdar, A. Characterization of Grafting Density and Binding Efficiency of DNA and Proteins on Gold Surfaces. *Langmuir* **2005**, *21*, 1956.
(33) Ray, S. G.; Cohen, H.; Naaman, R.; Rabin, Y. Where is the Sodium in Self-Assembled Monolayers of Single-Stranded DNA? *J. Am. Chem. Soc.* **2005**, *127*, 17138.
(34) Zhou, J.; Shu, W.; Welland, M. E.; Huck, W. T. S. Highly Reversible and Multi-Stage Cantilever Actuation Driven by Polyelectrolyte Brushes. *J. Am. Chem. Soc.* **2006**, *128*, 5326.
(35) Cai, P.; Huang, Q.; Li, M.; Liang, W. Binding and Degradation of DNA on Montmorillonite Coated by Hydroxyl Aluminum Species. *Colloids Surf., B* **2008**, *62*, 299.